Science Press

ARTICLE

Surface Temperature Field of Ti-6Al and Ti-48Al Alloys Under Continuous Laser Ablation

Sun Ruochen,   Mi Guangbao

Aviation Key Laboratory of Science and Technology on Advanced Titanium Alloys, AECC Beijing Institute of Aeronautical Materials, Beijing 100095, China

Abstract: The high temperature fire retardancy of titanium alloy is an important factor restricting its application in aero-engine, and the laser ignition method can accurately reflect the fire retardancy of titanium alloy under local heating. Due to the limitations of laser ignition experiments on the microscopic boundary and the transient propagation mechanism of the temperature field, molecular dynamics (MD) simulations and JMatPro calculation were applied to study the temperature field of Ti-6Al and Ti-48Al alloys. The results show that a molten pool is formed on the surface of Ti-Al alloys under continuous laser irradiation, and the temperature field of the molten pool is normally distributed from the center to the edge. When the center temperature reaches the critical point of ignition, the extended combustion occurs, and the extended combustion path advances along the direction of the air flow. Compared with Ti-6Al alloy, Ti-48Al alloy has higher fire retardancy under laser ablation. This is due to the better heat transfer performance of Ti-48Al, which leads to the weakening of the heat concentration effect near the boundary of the spot temperature field. So it is necessary to increase the partial pressure of oxygen, and thus to reduce the ignition point of the alloy in order to achieve the ignition boundary condition of Ti-48Al alloy under the same laser heat source. In the aspect of extended combustion path, the boundary heat collection effect of specimens shown by MD models reveals another mechanism affecting combustion expansion path besides the direction of air flow. That is, the heat generated by the laser spot is interrupted when it is transmitted to the boundary of the specimen along the short side direction, resulting in a concentration of heat near the boundary. So the combustion path also tends to expand along this direction.

Key words: Ti-Al alloys; laser ignition; molecular dynamics; temperature field

---

With the continuous progress of titanium (Ti) alloy materials, the utilization quantity of titanium alloy in aero-engine is also increased. Among them, Ti-Al alloys occupy a considerable proportion. Ti-Al alloy can maintain high specific strength and excellent creep resistance in high temperature service conditions, so it has become a potential high-temperature material. Ti alloy can be used for key components[1–2], such as high-pressure compressor blades, integral blades and casings, in order to achieve high mass reduction of advanced aero-engine.

In the process of application, the blades at all levels are the parts under the most severe working condition and the most complex load in the aero-engine. They are subjected to harsh conditions of high temperature and pressure. Therefore, the anti-oxidation and fire proof properties of Ti-Al alloys under

simulated high temperature environment have become the research focus in the Ti alloy field. It is revealed that an Al content of 6% is insufficient to form a continuous protective Al_2O_3 layer at the interface of the melting zone and heat affected zone[3]. Taking Ti-6Al-4V alloy as an example, the oxygen diffusion activation energy of the alloy at 600–800 °C is 202 kJ/mol, and the oxidation process conforms to the linear kinetic law[4]. The oxide layer of Ti-6Al-4V alloy can be roughly divided into three parts from the inside to the outside, including TiO_2, Al_2O_3 and $TiVO_4$[5]. With the continuous oxidation, a high density pore structure is generated inside the oxide layer and at the metal/oxide interface. At this moment, there is a certain number of O_2 molecules in it. At 500 °C, only 20% of O atoms exist in the oxide layer of the Ti-6Al-4V alloy, while at 600 °C, this value increases to 80%[6].

After accelerated oxidation by heat, the alloy reaches the ignition point and enters a stable combustion state, the temperature of burning zone can reach 2900 °C, and the combustion zone is melted. The ignition points of Ti-6Al-4V alloy at oxygen pressure of 0.1–0.4 MPa are 899–693 °C[7].

For the study of fire retardancy of titanium alloys, especially Ti-Al series, an effective method for the study of combustion properties of titanium alloys is indispensable. Based on the friction ignition theory, the friction-oxygen concentration ignition experiment is usually carried out with paired rotor and stator. It can effectively characterize the fire proof properties of TC11, TB12, TA15 and other Ti alloys[1,8–9]. This method to some extent is similar to the grinding condition of aero-engine, and is closer to the actual ignition condition. In addition to the friction method, another method to achieve heat accumulation and to make Ti alloy quickly ignite is called as the laser ignition method[10]. Different from the friction methods, the laser method can obtain the precise parameters of Ti alloy through the accurate control of the laser beam power, spot size and irradiation time, and the obtained test values have high accuracy. So it has great development potential and application value.

In addition to the traditional experimental testing and characterization methods, the simulation method based on numerical calculation also plays an important role in the study of laser ablation of metal surfaces. Finite element analysis (FEA) can realize the dynamic analysis of heat transfer and liquid phase fluid coupling during ablation of Ti-6Al-4V alloy[11]. On the micro-scale, the classical molecular dynamics (MD) and two-temperature model (TTM)-MD methods can be used to achieve femtosecond and nano-scale analysis of laser ablation. With the application of the MD method, Sachin[12] and Peng et al[13] adopted the temperature field data of the center and edge of the ablation zone calculated based on FEA as the parameters for MD simulation, and then revealed the temperature simulation of the semi-circular ablation zone and heat transfer zone with Langevin thermostat. In TTM-MD, MD is combined with a coupled factor system based on TTM algorithm to achieve heat conduction under thermal equilibrium and Fermi-Dirac distribution[14]. Yudi et al[15] adopted this method to study the sensitivity of the laser ablation process to the heating rate of the lattice. Gu et al[16] applied the multi-scale method (combined FEA and MD) to simulate the elastic and plastic deformation of TC4 alloy under laser irradiation, and further analyzed the influence of laser shock wave on the evolution of stress waves in TC4 alloy. According to relevant references about FEA and MD applied for laser ignition, it seems that the advantages of MD compared with FEA are mainly shown on two aspects: (1) the ability to capture changes on crystal or even lattice parameters; (2) the extremely short time step for power input by continuous laser.

At present, the comprehensive study of laser ignition method and characteristics of Ti-Al alloy is still in the early stage, and the research mainly focuses on the analysis of ignition resistance. However, the temperature field evolution

and microscopic mechanism of laser ignition are still unclear. For the continuous laser ignition time within 5 – 10 s, particularly the time difference of picosecond-level is enough to cause structural changes on the metal surface[14]. While under high temperature and high pressure ignition conditions, it is still difficult for traditional experimental methods to capture the change trend of microstructure and thermo-dynamic parameters in a very short time. So the relevant conclusions are still relatively limited. In addition, for Ti-Al alloys, the content of Al element has a potential effect on the thermal conductivity of the alloy, which indirectly determines the ignition characteristics of the alloy under continuous laser ignition. However, the current laser ignition experiment cannot focus on the temperature field difference at the microscopic boundary of the laser spot of Ti-Al alloy with different Al contents while researching the macroscopic ignition characteristics of the alloy.

In order to overcome the limitations of single macroscopic experiment or microscopic simulation in the study of laser ignition characteristics of Ti-Al alloy, and to clarify the mechanism of ignition and combustion expansion, this study adopted a combination approach of these two methods. Ti-6Al and Ti-48Al binary alloys were both taken as the research object. The microscopic mechanism affecting the boundary conditions and extended combustion path of Ti-6Al and Ti-48Al alloys was further revealed. Meanwhile, the influence of Al content on the heat transfer and initiation characteristics of Ti-Al alloys was further clarified. The data of this study will provide reference for composition optimization, fire proof improvement, mechanism analysis and extended combustion path prediction of Ti-Al alloys.

1 Methods

1.1 Laser ignition experiments

In order to obtain the typical characteristics of burning Ti-6Al and Ti-48Al alloys, the temperature field of laser ignitions was investigated. As shown in Fig. 1[10], the Ti alloy laser ignition experimental device consists of gas supply system, laser system, detection system and combustion chamber. The Ti-6Al and Ti-48Al alloys were placed in the combustion chamber, and the working environment under different air flow conditions such as temperature, flow rate and oxygen partial pressure was simulated by the gas supply system.

The alloy samples of Ti-6Al and Ti-48Al were flake
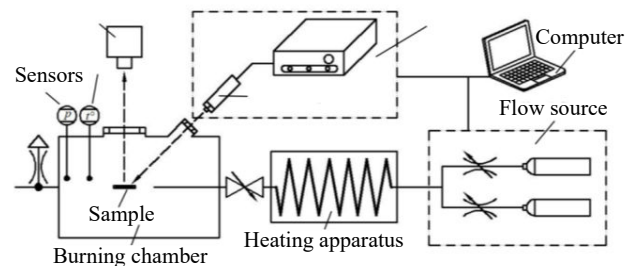
Fig.1   Ti alloy laser ignition experimental device

structure with smooth surface. There was no coating on the surface and the microstructure was uniform. The sample was in the shape of cylinder with 26 mm in diameter. The upper surface area for this cylinder sample was about 530.7 mm², the thickness of which was 2 mm. The laser spot conducted by fiber was irradiated at the edge of the sample, which is close to the direction of the inlet port. The temperature field data of the sample surface were obtained by the temperature sensor during the continuous laser ignition for 5 s and the subsequent free-extension combustion stage. During combustion, the inlet and outlet ports remain open, and the airflow speed and temperature remain constant.

1.2 MD simulations

With the continuous optimization of computational efficiency and interatomic motion control algorithm, the computational scale of MD simulation has been effectively improved[17]. This provides the feasibility for MD simulations of larger Ti-6Al and Ti-48Al alloys. The MD simulation method based on LAMMPS[18–19] program was adopted in this study. In terms of interatomic potential, the EAM force field developed by George Mason University was used[20], which combined the calculation efficiency and accuracy of metal element Ti-Al systems. The potential energy function of EAM force field is shown in Eq.(1)[21].

$$E_{\text{tot}} = \sum_i F_i(\phi_i) + \frac{1}{2}\sum_i\sum_{j \neq i}\varphi_{ij}(r_{ij}) \tag{1}$$

where E_{tot} is potential energy; F_i is embedding energy; ϕ_i is electron density of atom i; $\varphi_{ij}(r_{ij})$ is electrostatic interaction potential between atoms i and j; r_{ij} refers to position of atom i and j.

In terms of the geometry of Ti-6Al and Ti-48Al alloy models, a cubic structure with a size of 70 nm×30 nm×2 nm was adopted. Body-centered cubic (bcc) crystals with an initial lattice constant of 0.330 65 nm was set in models. As for the alloying models, the "type/ratio" algorithm in LAMMPS program was performed. As shown in Eq.(2), $Q_{\text{Ti/Al}}$ is the content (wt%) of Ti and Al atoms. When the total atomic number (N_{total}) of the Ti-Al alloy and the relative atomic mass ($M_{\text{Ti/Al}}$) of the Ti/Al elements are given, P_{Al} (atomic fraction, at%) of alloying element Al can be obtained according to Eq.(3). Then, on the basis of the original Ti-Al alloy models, all models were relaxed at 400 K for 2 ns. Finally, the Ti-6Al and Ti-48Al alloy models with minimized energy were obtained. Visualization of all models and analysis of all atomic properties in this study were based on OVITO[22] visualization program.

$$\frac{Q_{\text{Ti}}}{Q_{\text{Al}}} = \frac{N_{\text{Ti}}M_{\text{Ti}}}{N_{\text{Al}}M_{\text{Al}}} \tag{2}$$

$$P_{\text{Al}} = \frac{N_{\text{total}} - \dfrac{Q_{\text{Ti}}M_{\text{Al}}N_{\text{total}}}{Q_{\text{Al}}M_{\text{Ti}} + Q_{\text{Ti}}M_{\text{Al}}}}{N_{\text{total}}} \times 100\% \tag{3}$$

As shown in Fig. 2, two Ti-Al alloy (Ti-6Al and Ti-48Al) models with different proportions are simulated. In continuous laser ablation, the simulated spot diameter was 6 nm. The two models maintained a continuous heating rate of 3.4 K/ps in the spot region during the irradiation time of 500 ps. In addition,
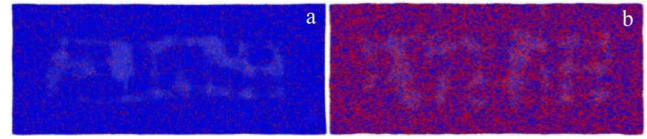
Fig.2   Initial models of Ti-6Al (a) and Ti-48Al (b) alloys

microcanonical ensemble (NVE) was applied for all models.

1.3 JMatPro calculations

The thermodynamic properties of Ti alloys are important physical parameters that affect the burning effect and ignition characteristics. The thermal conductivity and heat capacity of Ti-6Al, Ti-25Al and Ti-48Al binary alloys, whose composition is shown in Table 1, were calculated based on JMatPro (Version 7.0) program. Due to the change of element contents, Ti-6Al was solid solution Ti alloy, while Ti-25Al and Ti-48Al were intermetallic compounds. Calculation database was "Titanium Alloy" database of JMatPro program, and it was used for Ti-6Al and Ti-48Al alloys. Then, the Extended General tool under the Thermo-Physical Properties module was used to calculate the thermodynamic parameters of Ti-6Al and Ti-48Al alloys at different temperatures.

2 Results and Discussion

2.1 Laser ignition of Ti-6Al and Ti-48Al alloys

The phase composition of Ti-48Al is directly affected by the increase in the proportion of Al element. Compared with Ti-6Al alloy, with the increase in Al content, the alloy microstructure is transformed from α-Ti to Ti$_3$Al phase, and the thermal conductivity is changed. The thermal conductivity of the alloy directly affects the temperature field under laser ablation, and indirectly determines the ignition characteristics of the alloy. In order to compare and to analyze the temperature field characteristics of Ti-6Al and Ti-48Al alloys during ablation and extended combustion, the ignition characteristics of these two binary alloys were tested under continuous laser irradiation.

Table 2 and Fig. 3 show the ignition characteristic

Table 1   Element content of Ti-6Al and Ti-48Al alloys in JMatPro (wt%)

Alloy	Ti	Al
Ti-6Al	94.0	6.0
Ti-25Al	84.18	15.82
Ti-48Al	65.78	34.22

Table 2   Ignition characteristics of Ti-6Al and Ti-48Al alloys after continuous laser ablation at 275 W for 5 s

Alloy	C_O/%	Burnt area/mm²	Result
Ti-6Al	30	9.6	Ignited
	40	145.4	Ignited
Ti-48Al	70	0	Un-ignited
	78	202.7	Ignited
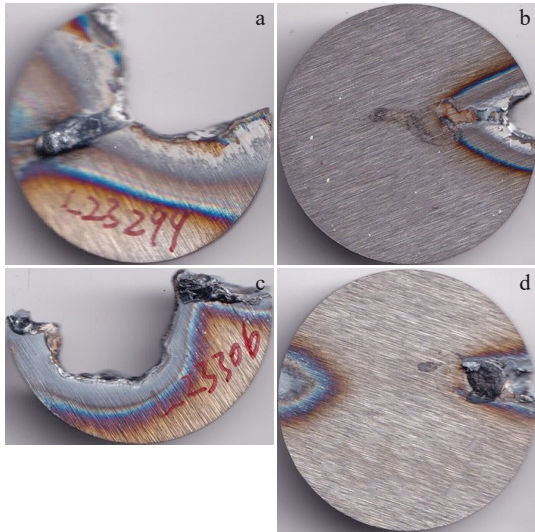
Fig.3   Ti-6Al (a−b) and Ti-48Al (c−d) alloys laser ablated at 275 W for 5 s under different oxygen partial pressure: (a) C_O=40%, (b) C_O=30%, (c) C_O=78%, and (d) C_O=70%

Fig.4   Extended combustion process of Ti-6Al and Ti-48Al alloys

comparisons of Ti-6Al and Ti-48Al alloys under different oxygen partial pressures (C_O) in continuous laser ablation at 275 W for 5 s. When the C_O of Ti-6Al alloy is 30%, it can be ignited, but the combustion sustainability is weak, and the combustion area is limited to the spot area, about 9.6 mm^2. When the C_O is increased to 40%, the combustion sustainability is enhanced, and the combustion area is a fan-shaped area of the 1/4 circle (145.4 mm^2). In contrast, Ti-48Al has higher flame retardant performance. Under the same laser heat source condition, as the C_O increases to 70%, the alloy remains un-ignited until the C_O increases to near 78%. In this condition, the ignition of Ti-48Al is achieved and the sample is burned through. The burnt area for Ti-48Al is as large as 202.7 mm^2.

Since a large number of sparks during intense combustion of Ti alloys are not conducive to the acquisition of optical images, the temperature field based on infrared thermal signals can characterize the complete ablation and combustion process. As shown in Fig.4, at the moment of laser irradiation (0−0.5 s), the spot center temperature of Ti-6Al and Ti-48Al alloys can reach 1300 – 1500 ° C. Under the same laser irradiation condition, the spot center temperature of Ti-6Al alloy is higher than that of Ti-48Al alloy. The Ti-6Al alloy produces a certain number of droplets in the air flow environment where C_O=30%. The peak temperature of the droplets is 2000 °C, and the droplets move along the direction of the air flow. At 1−2 s, the droplet cools and has a limited range of movement, so the ablation zone, as shown in Fig.3b, is confined to the vicinity of the light spot. When C_O increases to 40%, the expansion rate of melt droplets along the air flow direction is increased, and the persistence of extended combustion increases as well, which results in a fan-shaped ablation zone as shown in Fig.3a. The combustion sensitivity of Ti-48Al is lower than that of Ti-6Al. When C_O rises to 70%, the molten pool in the spot region is formed only at about
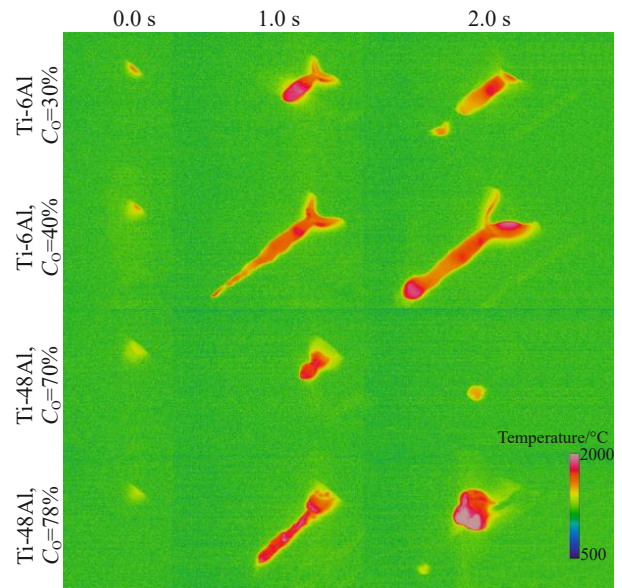
0.5 s. It is shown that the molten pool is not ignited or expanded. When the C_O further increases to 78%, the Ti-48Al alloy is ignited, which produces a large number of high temperature droplets along the airflow direction, and the combustion expands along the flow direction.

The temperature field characteristics of Ti-6Al alloy in the extended combustion stage after laser ignition are shown in Fig. 5. There are two peak temperature regions along the air flow direction (Line 1). The first one is the peak of the burning surface, and the peak temperature is about 2044 ° C.
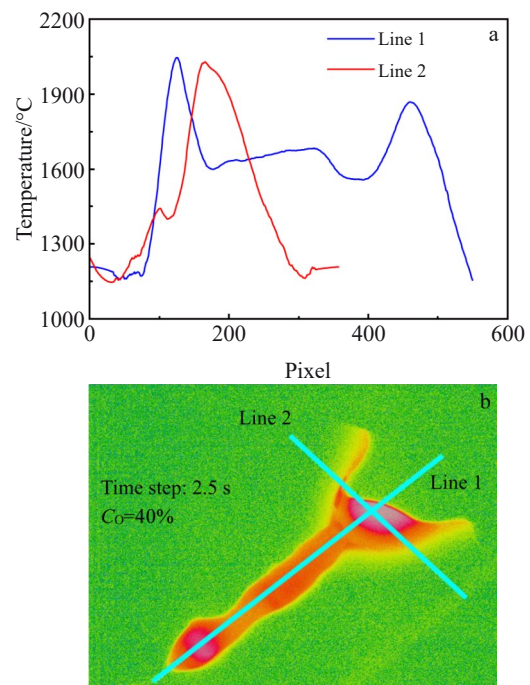
Fig.5   Temperature field distribution (a) and temperature graph (b) of Ti-6Al alloy with C_O=40%

The second peak is the droplet peak, and the peak temperature is about 1869 °C, which is slightly lower than the burning surface temperature. In the droplet movement path along the direction of the air flow, the temperature is 1600–1700 °C. Line 2 in Fig.5 shows that due to the high temperature of the burning surface, the unburned sample in the expansion path Line 2 is rapidly heated and then melted, and thus a new burning surface center is generated.

The temperature at the boundary of the burning surface is 1500–1600 °C, and the isotherm is evenly distributed. The temperature change rate from the center of the burning surface to the unburning area is basically the same, and the critical limit of the temperature increase is not shown. The temperature field of Ti-48Al alloy is shown in Fig.6. The laser ignition must be conducted in a high C_O environment due to the reduced combustion sensitivity. The higher the partial pressure of oxygen, the lower the ignition point of the alloy[23]. Therefore, Line 1 presents a multi-peak distribution with an average temperature of about 1800 °C. Along Line 2, the droplet path temperature of Ti-48Al is higher than that of Ti-6Al alloy.

2.2　MD simulation of Ti-6Al and Ti-48Al alloys

The temperature field evolution of Ti-6Al and Ti-48Al alloys during laser ablation and extended combustion process shows two main characteristics. (1) In terms of the expansion path after laser ignition, the disc sample generally expands in the sector region, rather than completely along the droplet movement direction. (2) In terms of combustion sensitivity, Ti-6Al alloy is significantly higher than Ti-48Al alloy. In other words, the content of Al element has a great influence on the ignition characteristics of the Ti-Al binary alloy. These two characteristics are closely related to the thermal conductivity of Ti-6Al and Ti-48Al alloys. In order to further reveal the microscopic mechanism, MD simulation models of Ti-6Al and Ti-48Al alloys are established from the perspective of heat transfer and temperature field analysis.
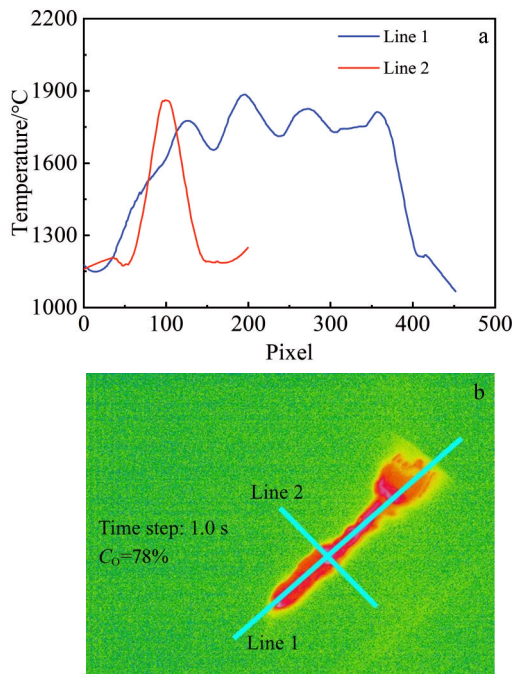
Taking the Ti-6Al alloy model as an example, the evolution process of temperature field during ablation in 0–500 ps continuous laser irradiation is shown in Fig.7. At 100, 200 and 300 ps, the core temperature of the spot is 640, 980 and 1320 K, respectively. At the same time, as the core is heated, the heat spreads around 360°, forming a gradient temperature field under the action of heat transfer. At 400 ps, the core temperature is 1660 K. Because the heat transfer space in the vertical direction is limited, it is relatively smaller than that in the horizontal direction. It can be seen that the heat concentration area is formed near the upper and lower edges of the model, and the temperature is higher than that of the left and right edges. Due to the low structural thermal stability of the nano-model in MD simulation, the heat concentration on the upper and lower edges leads to a phenomenon similar to necking. It seems that with the laser irradiation, the heat concentration of the Ti-6Al and Ti-48Al alloy samples along the short side direction (*Y*-axis) will be more obvious. In addition, as shown in Fig.8, there is also a certain range of liquid phase region outside the laser ablation boundary, and the temperature of this region is 1200–1300 °C. Under the heat concentration effect of the upper and lower boundaries, the liquid phase region outside the spot boundary will penetrate the upper and lower boundary regions.

This result shows that the morphology of laser ignition sample has great influence on its heat transfer distribution. When the heat is transferred to the boundary near the spot, the heat conduction is blocked, resulting in the heat concentration, the temperature increase rate is accelerated, and the expansion of the combustion path is more inclined to this direction. In the sample shown in Fig.3, heat concentration also tends to the direction near the boundary of the light spot, resulting in the phenomenon of spreading combustion along the fan-

Fig.6　Temperature field distribution (a) and temperature graph (b) of Ti-48Al alloy with C_O=78%
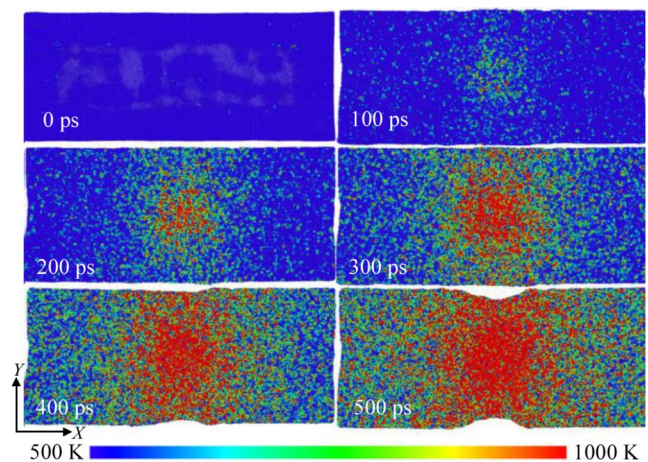
Fig.7　Temperature field changes of Ti-6Al alloy in continuous laser heating process at different moments
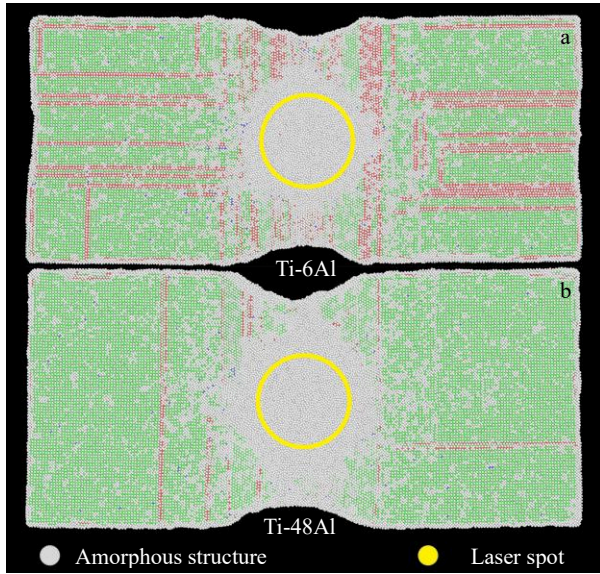
Fig.8 Phases of Ti-6Al (a) and Ti-48Al (b) alloys at 500 ps

Fig.9 Horizontal temperature field distributions of Ti-6Al (a) and Ti-48Al (b) alloys

Fig.10 Radial temperature field distribution of Ti-6Al and Ti-48Al alloy near laser ablation boundary

shaped area.

In terms of the effect of Al content on the heat transfer performance of the alloy, the analysis method of spot boundary temperature gradient contrast can be applied. Fig. 9 shows the temperature field distribution of Ti-6Al and Ti-48Al alloys along the long side direction (X-axis). The temperature field changes of Ti-6Al and Ti-48Al alloys from the ablative center to the edge basically conform to the normal distribution law, which is consistent with the test results in Fig.5, proving the effectiveness of MD simulation for the ablative temperature field. When the core temperature of the spot is about 1850 °C, the spot boundary temperature of Ti-6Al and Ti-48Al alloys is basically close, 1210−1250 °C. Compared with that of Ti-6Al, the ratio of Ti and Al elements in Ti-48Al alloy is close, so the temperature curves basically coincide, and Ti is the main element in Ti-6Al alloy. Thus, its temperature curve in the ablation temperature field is slightly higher than that of Al element.

The temperature field gradient of Ti-6Al near the spot boundary is −88 K/nm, while that of Ti-48Al is −110 K/nm, which is attributed to the higher thermal conductivity of Ti-48Al, so the heat at the spot boundary can be conducted more effectively to the non-ablative surface, thereby reducing the spot boundary temperature. Fig. 10 shows the radial temperature of Ti-6Al and Ti-48Al alloys within ±0.3 nm of the spot boundary, with the geometric center of the spot as the origin. Within the spot boundary, the basic temperature field shows a linearly decreasing trend, and the temperature of Ti-6Al is slightly higher than that of Ti-48Al alloy. Because Ti-48Al alloy has higher thermal conductivity, the temperature near the spot boundary is slightly lower than that of Ti-6Al alloy. Since heat concentration and rapid temperature rise in the laser ablation process are the prerequisite for the ignition of Ti alloy, the improvement of thermal conductivity is not conducive to the heat concentration near the spot boundary, so
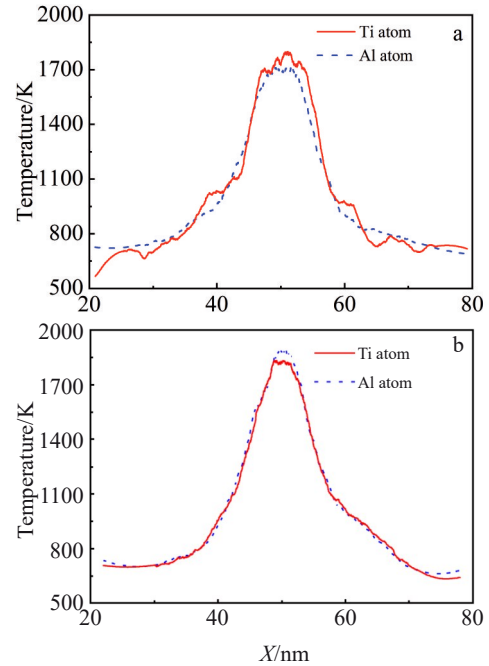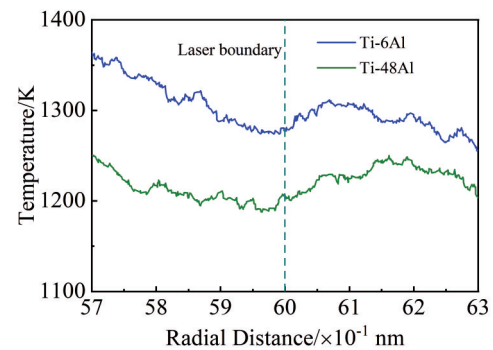
Ti-48Al alloy shows lower combustion sensitivity and higher flame retardant performance in the laser ablation ignition experiment.

2.3 Thermal conductivity and heat capacity

In the calculation of Ti-Al alloy properties, the prediction model based on JMatPro shows good applicability[24]. In terms of thermal conductivity and heat capacity calculation, according to the MatWeb database, the thermal conductivity of Ti-6Al-4V alloy at 650 °C is 17.5 W/(m·K)⁻¹, while the heat capacity at 870 °C is 0.930 J/(g·°C)⁻¹. For Ti-6Al-4V alloy, the calculated values of the thermal conductivity and heat capacity are 17.01 W/(m·K)⁻¹ and 1.13 J/(g·°C)⁻¹, respectively, so the deviation for these two parameters is only − 0.49 W/(m·K)⁻¹ and 0.2 J/(g·°C)⁻¹, respectively. This suggests that the JMatPro calculation is also valid for the calculation of thermal conductivity and heat capacity under high temperature

ablative environment.

According to MatWeb data, the thermal conductivity of Ti is 17 W/(m·K)$^{-1}$, and that of Al is 210 W/(m·K)$^{-1}$ which is much higher than that of Ti. Therefore, in Ti-Al binary alloy system, the Al content will have a great influence on the overall thermal conductivity of the alloy. As shown in Fig.11, when Al content increases from 6% to 48% at 600 °C, the thermal conductivity of the alloy increases by about 2.96 times. When the temperature rises further, the increase extent of thermal conductivity becomes lower. This is because the melting point of Al is 660.37 °C, which is lower than that of Ti (1650 °C). When the content of Al is high, the motion amplitude of Al atom at high temperature is intensified, which accelerates the heat transfer. Therefore, the influence of Al content on thermal conductivity at high temperature is relatively weak. In terms of the influence of heat capacity, although the heat capacity also increases with the addition of Al, the change amplitude is relatively not obvious.

JMatPro calculation results indicate that the difference in thermal conductivity of Ti-6Al, Ti-25Al and Ti-48Al alloys at 600 °C is greater than that in state parameter at 1800 °C. In other words, the difference of thermal conductivity under different Ti/Al ratios decreases with the increase in temperature. Therefore, in the laser ablation ignition experiment, although the laser ablation ignition performance of Ti-48Al alloy is much different from that of Ti-6Al alloy, the temperature field difference in the extended combustion stage is larger due to the increase in oxygen partial pressure caused by the increase in C_O. Then, the burning intensity and persistence of Ti-48Al alloy are largely increased.
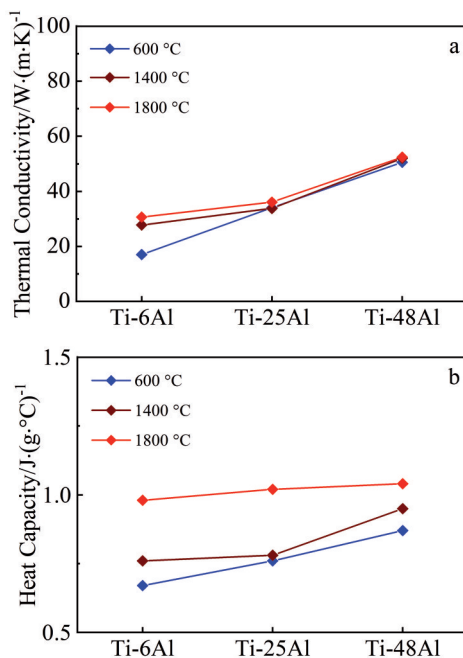
Fig.11   Thermal conductivity (a) and heat capacity (b) of Ti-6Al, Ti-25Al and Ti-48Al alloys

3 Conclusions

1) In the process of continuous laser ablation, Ti-6Al and Ti-48Al alloys firstly form a molten pool within the spot range. The center temperature of the molten pool is above 1600 °C, the edge temperature is slightly lower, and the overall distribution meets normal distribution. The heat at the edge of the molten pool diverges to all sides, forming a liquid phase region with a range larger than the light spot. Compared with Ti-6Al, the combustion sensitivity of Ti-48Al alloy is lower, and the critical ignition C_O of Ti-48Al alloy is 70%－78% under the laser ablation at 275 W for 5 s, which is much higher than the critical ignition C_O of Ti-6Al alloy.

2) The geometric morphology of the sample is an important factor affecting the combustion expansion path, because the heat will be concentrated near the boundary of the light spot. As a result, the temperature increase rate is accelerated, the atomic thermal motion is intensified, and thus the titanium alloy surface along the path is more easily ignited. Therefore, Ti-6Al and Ti-48Al alloys are burned in the fan direction after laser ablation.

3) The influence of Al ratio on the ignition characteristics of Ti-Al binary alloy is partly due to the change of thermal conductivity of the alloy. When the proportion of Al element in Ti-Al binary alloy is increased, the thermal conductivity of the alloy is improved, and the heat concentration effect at the spot boundary in continuous laser irradiation is weakened, which is helpful to improve the critical condition of ignition of Ti-Al binary alloy. Compared with Ti-6Al alloy, the critical ignition C_O of Ti-48Al is higher under the same heat source.

References

1   Mi Guangbao, Huang Xu, Cao Jingxia *et al. Transactions of Nonferrous Metals Society of China*[J], 2013, 23(8): 2270

2   Ouyang Peixuan, Mi Guangbao, Cao Jingxia *et al. Materials Today Communications*[J], 2018, 16: 364

3   Wu Mingyu, Mi Guangbao, Li Peijie *et al. Acta Physica Sinica*[J], 2023, 72(16): 166102 (in Chinese)

4   Hasan Guleryuz, Huseyin Cimenoglu. *Journal of Alloys and Compounds*[J], 2009, 472: 241

5   Rajabi A, Mashreghi A R, Hasani S. *Journal of Alloys and Compounds*[J], 2020, 815: 151948

6   Antoine Casadebaigt, Jonathan Hugues, Daniel Monceau. *Corrosion Science*[J], 2020, 175: 108875

7   Shao Lei, Xie Guoliang, Liu Xinhua *et al. Corrosion Science*[J], 2022, 194: 109957

8   Sui Nan, Mi Guangbao, Yan Mengqi *et al. Rare Metals*[J], 2018, 37(11): 952

9   Mi Guangbao, Cao Chunxiao, Huang Xu *et al. Journal of Aeronautical Materials*[J], 2014, 34(4): 83 (in Chinese)

10   Mi Guangbao, Chen Hang. *Chinese Patent*, ZL201711188505.5[P], 2017 (in Chinese)

11   Zhao Wen, Yu Zhou, Hu Jun. *Journal of Manufacturing Processes*[J], 2023, 99: 138

12 Sachin Kurian, Reza Mirzaeifar. *Additive Manufacturing*[J], 2020, 35: 101272

13 Peng Kaiyuan, Huang Haihong, Xu Hongmeng. *International Journal of Mechanical Sciences*[J], 2023, 243: 108034

14 Guo Jianwu, Ji Pengfei, Jiang Lan *et al. Powder Technology*[J], 2022, 407: 117682

15 Yudi Rosandi, Herbert M Urbassek. *Applied Physics A*[J], 2013, 110: 649

16 Gu Cheng, Su Minghua, Tian Zenghui *et al. Optics & Laser Technology*[J], 2023,165: 109629

17 Wang Yan, Liu Tianjiao, Xie Jinhui. *Current Research in Food Science*[J], 2022, 5: 1873

18 Steve Plimpton. *Journal of Computational Physics*[J], 1995, 117(1): 1

19 Thompson A P, Metin A H, Richard B *et al. Computer Physics Communications*[J], 2022, 271: 108171

20 Zope R R, Mishin Y. *Physical Review B*[J], 2003, 68: 024102

21 Vella J R, Stillinger F H, Panagiotopoulos A Z *et al. Journal of Physical Chemistry B*[J], 2015, 119: 8960

22 Alexander Stukowski. *Modeling and Simulation in Materials Science and Engineering*[J], 2010, 18: 1

23 Bolobov V I. *Combustion, Explosion and Shock Waves*[J], 2002, 38: 639

24 Xu Jiajia, Wang Fei. *Hot Working Technology*[J], 2018, 47(10): 72 (in Chinese)

连续激光烧蚀作用下Ti-6Al与Ti-48Al合金表面的温度场

孙若晨，弭光宝

(中国航发北京航空材料研究院 先进钛合金航空科技重点实验室，北京 100095)

摘　要：钛合金的高温阻燃性能是制约其在航空发动机中应用的重要因素，而激光点火法能够精确反映钛合金在局部加热时的阻燃性能。在Ti-6Al与Ti-48Al的温度场研究中，通过钛合金激光点火实验表征了温度场演化特性，同时在微观瞬态机制分析中引入了分子动力学（MD）模拟与JMatPro计算等方法。结果表明：在激光连续照射下，Ti-Al系合金表面首先形成熔池，熔池温度场从中心到边缘呈正态分布。当中心温度达到起燃临界点时，产生扩展燃烧，扩展燃烧路径沿气流方向推进。与Ti-6Al相比，Ti-48Al合金在激光烧蚀下的阻燃性能更高。这是由于Ti-48Al具有更高的传热性能，导致光斑温度场边界附近的热集中效应减弱，因此需要增加氧分压，降低合金起燃点，才能在同等激光热源下达到Ti-48Al合金的起燃边界条件。另外在扩展燃烧路径方面，MD模型显示试件存在边界热集中效应，这揭示了除气流方向之外的另一种扩展燃烧路径影响机制，即激光光斑产生的热量传导至临近边界时中断，在边界附近产生热量集中，因此燃烧路径亦倾向于沿该方向扩展。

关键词：钛铝合金；激光点火；分子动力学模拟；温度场

作者简介：孙若晨，男，1992年生，博士，中国航发北京航空材料研究院先进钛合金航空科技重点实验室，北京 100095，电话：010-62496627，E-mail：sunrc836@qq.com